Learning to learn: Single session acquisition of new rules by freely-moving mice

Amir Levi[1,2], Noam Aviv[1], and Eran Stark[1,2]

[1] Department of Physiology and Pharmacology, Sackler School of Medicine, Tel Aviv University, Tel-Aviv 6997801, Israel

[2] Sagol School of Neuroscience, Tel Aviv University, Tel-Aviv 6997801, Israel

Correspondence: eranstark@tauex.tau.ac.il

Abstract

Learning from examples and adapting to new rules are fundamental attributes of human cognition. However, it is unclear what conditions allow for fast and successful learning. To determine how rapidly freely-moving mice can learn a new rule, we designed a fully automated two-alternative forced choice visual discrimination paradigm in which the rules governing the task can change between sessions. We find that animals can learn a new rule during the very first block of trials. The propensity for single session learning improves over time and can be accurately predicted based on animal experience and rule difficulty. When conditions for generalization from a previous rule are more favorable, mice perform single session learning with higher success rates. Units recorded from hippocampal region CA1 during a previously-learned visual rule exhibit task-related place fields and state-dependent modulation. A mouse trained on visual rules can learn an intra-cortical rule, generated by direct activation of hippocampal CA1 pyramidal cells. Thus, after establishing procedural learning of a paradigm, mice continue to perform and improve at associative operant learning of new rules.

Introduction

Solving a discrimination task for a reward and driving a car involve associative operant learning[1]. Through experience, we learn the relationship between stimuli, actions, and results, aligning our actions with the desired outcomes. As we practice the driving task, certain aspects become easier and are performed unconsciously. Thus, driving becomes procedural, a thing of habit[2,3]. Habit-like behavior is generated by extensive training[4,5]. Akin to humans, an animal trained on the same task for many days is expected to begin acting out of habit. Now consider traveling from a country where one is required to stop at a red light to a country where right turn on red is allowed. Suddenly, some of the rules of the well-known task have changed. The ability to learn from a small training set and adapt to new rules is a fundamental attribute of human cognition[6]. However, it is unclear how quickly animals learn new rules that govern a well-known task, and what conditions allow fast and successful learning.

One way to learn a new rule governing a well-known discrimination task is to generalize from a previously known rule. Rodents can use generalization[7] and transfer[8,9] to learn new rules. However, generalization cannot be used when a new rule is uncorrelated with a previously learned rule (recall the red-light example). A second option for successful performance when the rules change is categorization, an established ability among rodents[10,11]. However, new rules do not necessarily fall into previously

acquainted categories. Third, higher levels of attention and experience may facilitate faster learning[12]. Consider driving in yet another country and arriving at a traffic light junction. Experience from the previous two settings suggests looking for possible new rules. Indeed, attending to details increases learning rate[13].

Fast and one-shot learning[14] were demonstrated in laboratory rodents. In fear conditioning, a stimulus is associated with a single exposure to an aversive experience, leading to avoidance learning[15,16]. However, reconsidering the driving analogy, classical conditioning is more akin to learning to avoid going on red after an accident, compared to learning new rules (operant learning). Rodents also excel in spatial learning[17,18] and can learn from a single spatial experience, as with the Morris water maze[19-21]. However, spatial (episodic) learning and operant (associative) learning are associated with distinct neuronal mechanisms[22,23]. Furthermore, operant learning tasks take weeks to learn when conducted with head-fixed[24-26] or freely-moving[10,27,28] rodents. Thus, how rapidly rodents can learn a new discrimination rule within a well-known setting is still unknown.

Using a fully automated two-alternative forced choice (2AFC) paradigm, we find that every mouse learns a new visual discrimination rule in a single session. When single session learning (SSL) occurs, mice perform the task successfully from the first block. More experienced mice are more likely to perform SSL. SSL can be achieved for particularly difficult rules if conditions for generalization from previously learned rules are favorable. Units recorded from hippocampal region CA1 while a mouse performs a previously-learned visual rule exhibit task-related place fields and state-dependent modulation. Finally, we find that a mouse trained on the visual task can learn an intra-cortical rule. Thus, mice learn to learn.

Results

Mice can learn a new visual rule within a single session

We designed a fully automated 2AFC discrimination task for freely-moving mice in a T-maze (**Fig. 1A**). All subjects were hybrid mice pretrained ("shaped") over several days (median [interquartile range, IQR]: 5 [4 5] days). To maximize learning rate and minimize frustration, every session was divided into blocks (**Fig. 1B**). Each block consisted of five training trials followed by ten testing trials. During training trials, the subjects were presented with the same stimuli as during testing trials, but the correct choice was enforced by opening only one door at the T-junction (**Fig. 1C**). Mice received a water reward after every training trial and every successful testing trial.

During visual discrimination sessions, a display of 100 green and blue LEDs was used to generate a rule (**Fig. 1A, inset**). In every session, a single rule composed of two distinct visual cues {A; B} governed the task. Mice were tested on the ability to learn the stimulus-response association, i.e., the affinity between {A; B} and {go left; go right}. The physical properties of the two cues allowed characterizing every rule by an intra-rule distance that ranges [0,1] and is smaller for more difficult rules (**Fig. 1D**). For example, rule#1 consisted of {cue A: all green LEDs are on; cue B: all blue LEDs are on}, and had an intra-rule distance of 0.07.

Among other factors, animal response time is correlated with experience[29] and attention[12]. Here, response time was defined as the period from crossing the home box photosensor to lateral arm photosensor (**Fig. 1C**). Response times were anti-correlated with session ordinate (i.e., the 1st, 2nd, … session that the mouse encountered; rank correlation coefficient, cc: -0.11; n=5996 trials; p<0.001,

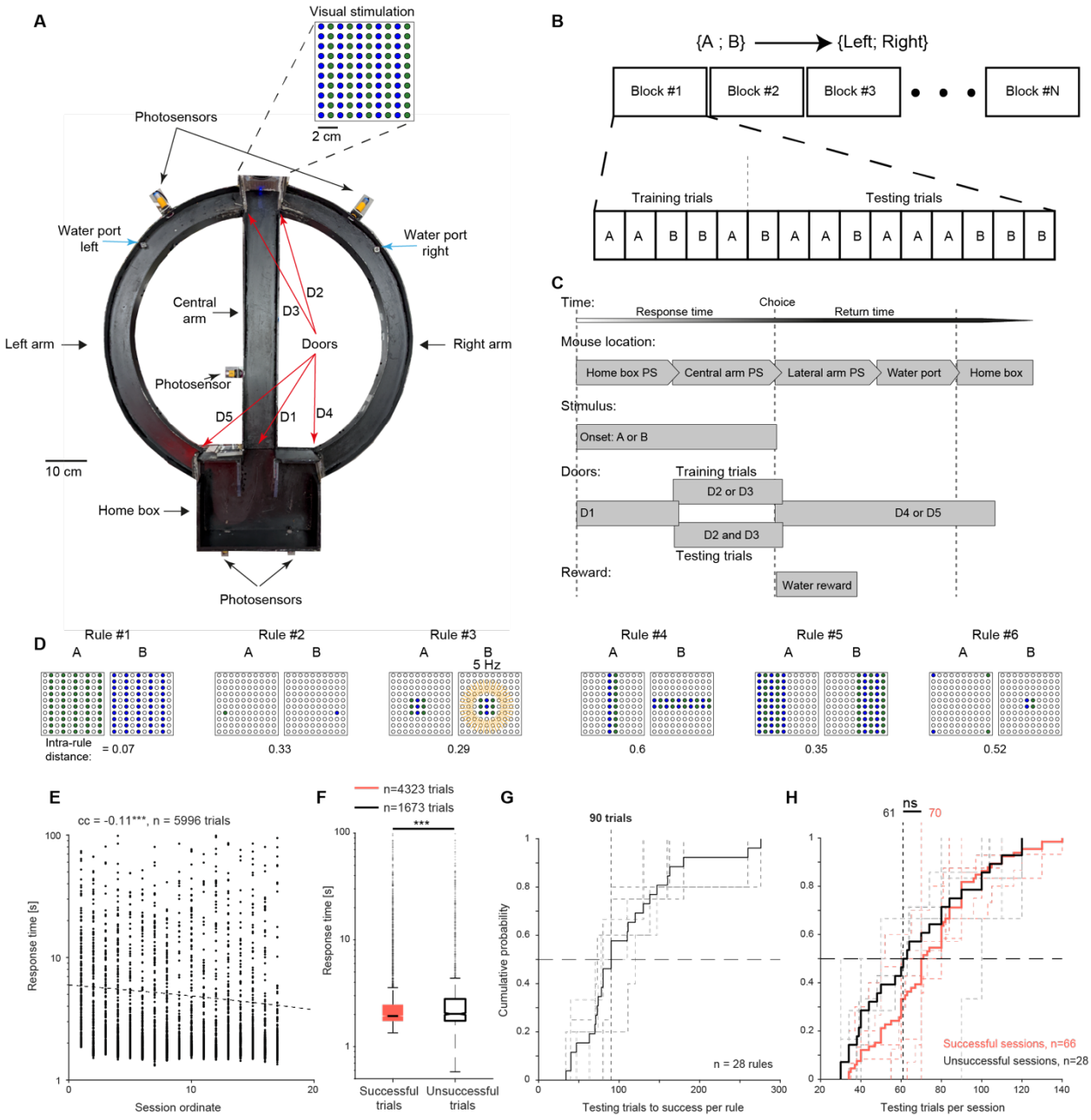

Figure 1. Mice learn a new visual rule within a single session. (**A**) The fully automated apparatus used to train freely-moving mice on a 2AFC discrimination task. Successful trials are reinforced by water. **Top**, The display used to generate visual rules, located at the far end of the central arm, consists of ten alternating columns of green and blue LEDs. (**B**) Session structure. Every session is composed of blocks, each consisting of five training followed by ten testing trials. (**C**) Trial structure. During training trials, only the correct choice is available to the animal since only one door at the T-junction is open (D2 or D3). (**D**) Six visual rules are used to govern the task. On every session only one rule is used. **Bottom**, The physical properties of two visual cues {A; B} are used to derive an intra-rule distance metric, quantifying rule difficulty. (**E**) Response times are correlated with animal experience. Dashed line, linear model fit. cc, rank correlation coefficient. ***: p<0.001, permutation test. (**F**) Response times are shorter during successful compared with unsuccessful testing trials. Every box plot shows median and IQR, whiskers extend for 1.5 times the IQR in every direction, and a plus indicates an outlier. ***: p<0.001, U-test. (**G**) Mice learn a new rule within a median of 90 testing trials. Here and in **H**, data are from six mice tested on 28 rules. Dashed lines, individual mice. (**H**) The number of testing trials performed during successful and unsuccessful sessions are not consistently different. ns: p>0.05, U-test.

permutation test; **Fig. 1E**). Furthermore, response times and success rates were anti-correlated (cc: -0.11; p<0.001). Response times during successful testing trials were 1.9 s [1.7 2.5] s (median [IQR]; n=4323 trials), lower than during unsuccessful trials (2 s [1.7 2.8] s; n=1673 trials; p<0.001, U-test; **Fig. 1F**). Return times to the home box were longer during successful trials (p<0.001, U-test), consistent with lingering at the reward ports. Thus, mouse response times depend on both experience and success rate.

Sessions were denoted as successful if performance was consistently above chance (0.5; p<0.05, Binomial test). A rule was deemed successfully learned if a successful session was performed while the task was governed by the rule. Using the six-rule pool (**Fig. 1D**), six mice were tested on 28 rules, with every mouse exposed to a median [IQR] of 5 [3 5] rules. When exposed to a new rule, 90 [70 138] testing trials were required to perform the task successfully (**Fig. 1G**). The number of testing trials during successful sessions was 70 [55 90] (n=66 sessions), not consistently different from unsuccessful sessions (61 [40 84]; n=28; p=0.16, U-test; **Fig. 1H**). The median number of testing trials during successful sessions was lower than 90, the median number of testing trials required to learn a novel rule (p<0.001, Wilcoxon's test). Yet the number of trials was above 90 in 16/66 (24%) of the successful sessions, suggesting that a new rule could be learned during a single session. Indeed, in 13/22 (59%) of the new rules encountered, the mice performed SSL. Thus, mice can learn a new visual rule within a single session.

During SSL, mice achieve high success rates from the first block

All six mice achieved SSL of at least one rule. For example, after pretraining on rule#2, mouse#3 (m3) performed the task successfully during the second and third testing sessions (**Fig. 2A**). The rule was then changed to rule#4, which was learned in a single session. m3 was tested on three new rules and achieved SSL on two. Overall, 5/6 (83%) rules were learned in one session by at least one mouse. The exception was rule#1, the most difficult rule employed (intra-rule distance, 0.07). Overall, 66/94 (70%) of the sessions were successful, with a median [IQR] success rate of 0.7 [0.6 0.8] (n=508 blocks), consistently higher than unsuccessful sessions (0.5 [0.4 0.6]; n=199; p<0.001, U-test; **Fig. 2B**).

We classified sessions according to the learning process. Each session was associated with either SSL (e.g., m4, rule#6; **Fig. 2C**), multi-session learning (MSL; e.g., m4, rule#2; **Fig. 2D**), or unlabeled (e.g., m4, rule#1). By definition, a rule associated with MSL requires more than one session to learn. Since every mouse was pretrained on the first rule, all first-rule sessions were unlabeled. Of the newly-encountered rules, 13/22 (59%) were SSL, 8/22 (36%; spanning 19 sessions) were MSL, and in one case the rule was not learned (1/22, 5%; m5, rule#1; **Fig. 2A**). Thus, in 95% of the cases, mice learn a completely new rule within one to three sessions.

Response times during SSL and MSL did not differ consistently (p=0.74, U-test; **Fig. 2E**). However, the correlation between response times and success was higher during SSL (cc: -0.1; n=973 trials; p=0.0012, permutation test) compared with MSL trials (cc: -0.06; n=1287; p=0.029). Furthermore, SSL success rates (0.7 [0.6 0.8]; n=110 blocks) were higher than MSL success rates (0.6 [0.5 0.7]; n=154; p<0.001, U-test; **Fig. 2F**). To quantify differences in the learning process, a linear model was fit to every SSL and MSL learning curve (**Fig. 2CD**, colored lines). During MSL, mice exhibited gradually increasing success rates (median slope: 1.3% improvement per block; n=8 rules; p=0.008, Wilcoxon's test comparing to a zero-slope null; **Fig. 2G, top left**). MSL initial success rates were not consistently different from chance (50%; median: 46%; p=0.055; **Fig. 2G, bottom left**). In contrast, SSL initial success rates were already above

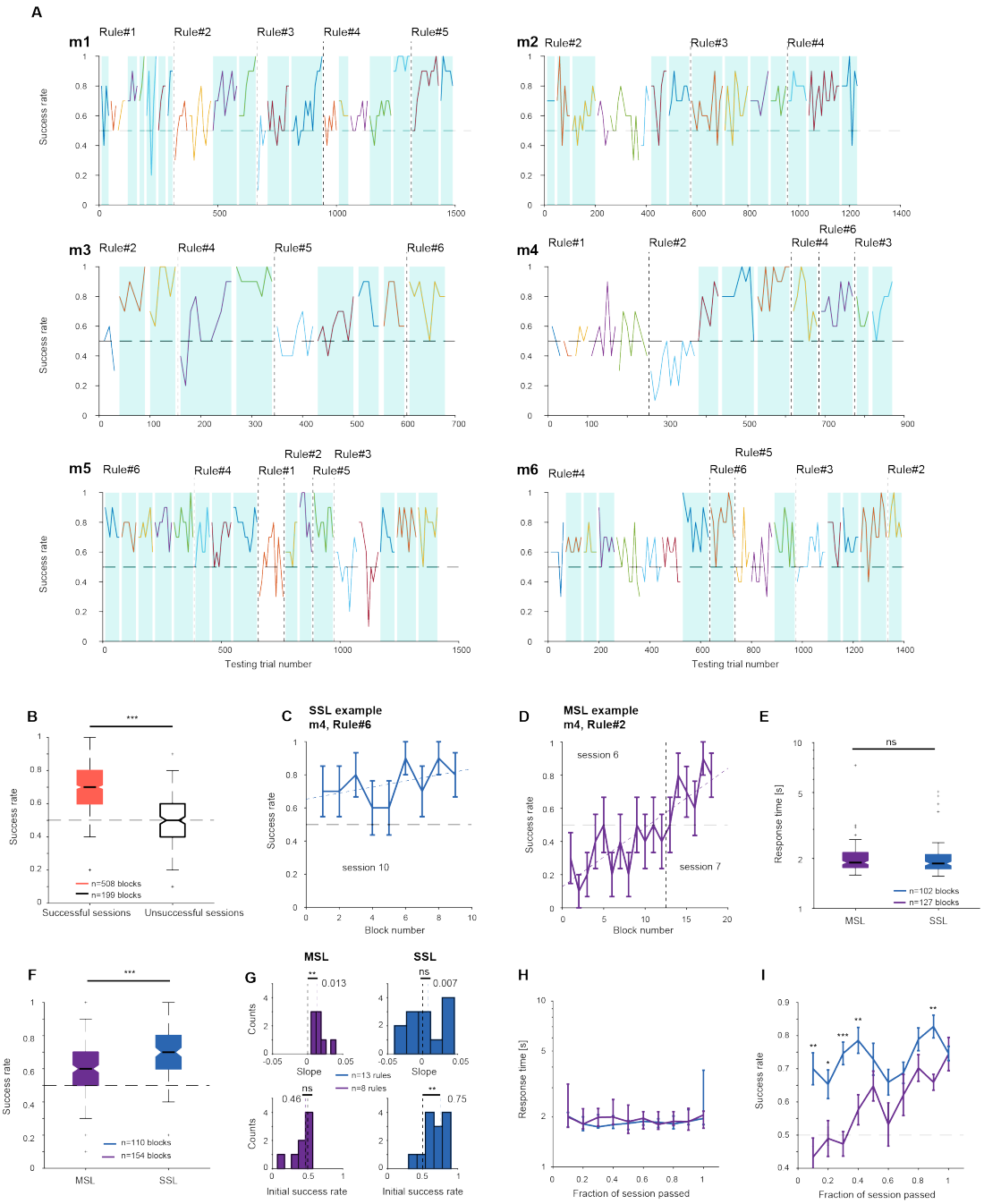

Figure 2. During SSL, mice achieve high success rates from the first block. (**A**) Success rate as a function of testing trial number for every mouse. Sessions are represented by distinct colors, and every point indicates single-block success rate. A blue background highlights successful sessions ($p<0.05$, Binomial test comparing to chance level, 0.5). (**B**) Success rates are higher during successful compared with unsuccessful sessions. Here and in **E, F,** and **I**, ns/*/**/***: $p>0.05/p<0.05/p<0.01/p<0.001$, U-test. (**C**) Example SSL curve. Here and in **D**, colored lines represent linear model fit. (**D**) Example MSL curve. (**E**) Response times are not consistently different between blocks during rules involving SSL and MSL. (**F**) Success rates are higher for SSL compared with MSL rules. (**G**) A linear model was fit to every learning curve. **Top**, MSL but not SSL curves have slopes consistently above zero. **Bottom**, SSL but not MSL curves have initial success rates consistently above chance. ns/**: $p>0.05/p<0.01$, Wilcoxon's test. (**H**) Response times of rules involving SSL and MSL are not consistently different at different points along the session. For all points, $p>0.05$, U-test. (**I**) Success rate of SSL is consistently higher compared to MSL during the initial 40% of the session.

chance (75%; n=13; p=0.003), and did not increase consistently (median slope: 0.7%; p=0.5; **Fig. 2G, right**). Thus, when SSL occurs, the trials experienced during the first block suffice for learning the new rule.

Linear models do not necessarily capture differences between learning curves. Instead of considering models that require more free parameters (e.g., sigmoid), we time-warped every curve to unity duration and averaged all learning curves of a given type (SSL or MSL; **Fig. 2HI**). SSL and MSL response times did not differ consistently during any tenth of the duration (p>0.05, U-test; **Fig. 2H**). However, success rates during the initial four tenths were higher for SSL compared with MSL sessions (geometric mean, p=0.004, U-test; **Fig. 2I**). The observations complement the linear model fit results, showing that during SSL animals learn the new rule during the very first block.

Single session learning can be predicted based on experience and rule difficulty

To assess what determines SSL, we first examined how rule identity affects success rates. Mice exhibited different success rates on different rules (**Fig. 3A**). For instance, rule#6 (**Fig. 1D**) yielded the highest success (0.8 [0.7 0.9]; n=65 blocks; geometric mean of five comparisons, p=0.00007, Kruskal-Wallis test; **Fig. 3A**). In contrast, rule#1 yielded the lowest success rates (0.6 [0.5 0.7]; n=67; p=0.006; **Fig. 3A**). Thus, success rates depend on the specific rule.

When the rule is replaced, mice are compelled to learn the specific new rule, requiring reference memory[30-33]. Other aspects of the task involve long-term memory and may be learned over multiple sessions. We found that success rates correlated with the session ordinate (cc: 0.14; n=736 blocks; p<0.001, permutation test; **Fig. 3B**). Correlation was higher when only the first sessions involving SSL and MSL were included (cc: 0.21; n=179 blocks; p=0.0043; **Fig. 3B, inset**). Thus, when mice are more experienced, performance is better when encountering a new rule.

Even if experience contributes to successful performance, rule difficulty may influence success rate. Based on the physical properties of the cues, rule difficulty was quantified using the intra-rule distance metric (**Fig. 1D**). Success rates correlated with intra-rule distance (cc: 0.12; p=0.002, permutation test; **Fig. 3C**). Higher correlation was observed when only the first SSL and MSL sessions were considered (cc: 0.28; p<0.001; **Fig. 3C, inset**). Thus, success rates are correlated with intra-rule distance, especially when a new rule is encountered.

Another possible route to successful performance is generalization from a previously-learned rule. If mice generalize, higher similarity between consecutively-presented rules may yield better performance, and grossly distinct rules may induce confusion. We quantified the similarity between every two rules using the inter-rule distance metric, which is near zero when rules are very similar and near one when rules are very different from one another. Success rate was anti-correlated with inter-rule distance (cc: -0.16; n=190 first-session blocks; p=0.03, permutation test; **Fig. 3D**). Similar results were obtained when only MSL and SSL first-session blocks were considered (cc: -0.17; p=0.023; **Fig. 3D, inset**). Thus, when the new rule is more similar to the previously-learned rule, success during the first session is already higher.

Based on the foregoing, success level depends on several possibly correlated features, including session ordinate (**Fig. 3B**), rule difficulty (**Fig. 3C**), and inter-rule similarity (**Fig. 3D**). We used partial correlation analysis to disambiguate the features. The partial rank correlation coefficient (pcc) was consistently distinct from zero for the session ordinate (pcc: 0.26; n=179 first-session blocks during MSL and SSL; p<0.001, permutation test; **Fig. 3E**) and for intra-rule distance (pcc: 0.34; p<0.001), but not for inter-rule distance (pcc: -0.15; p=0.052).

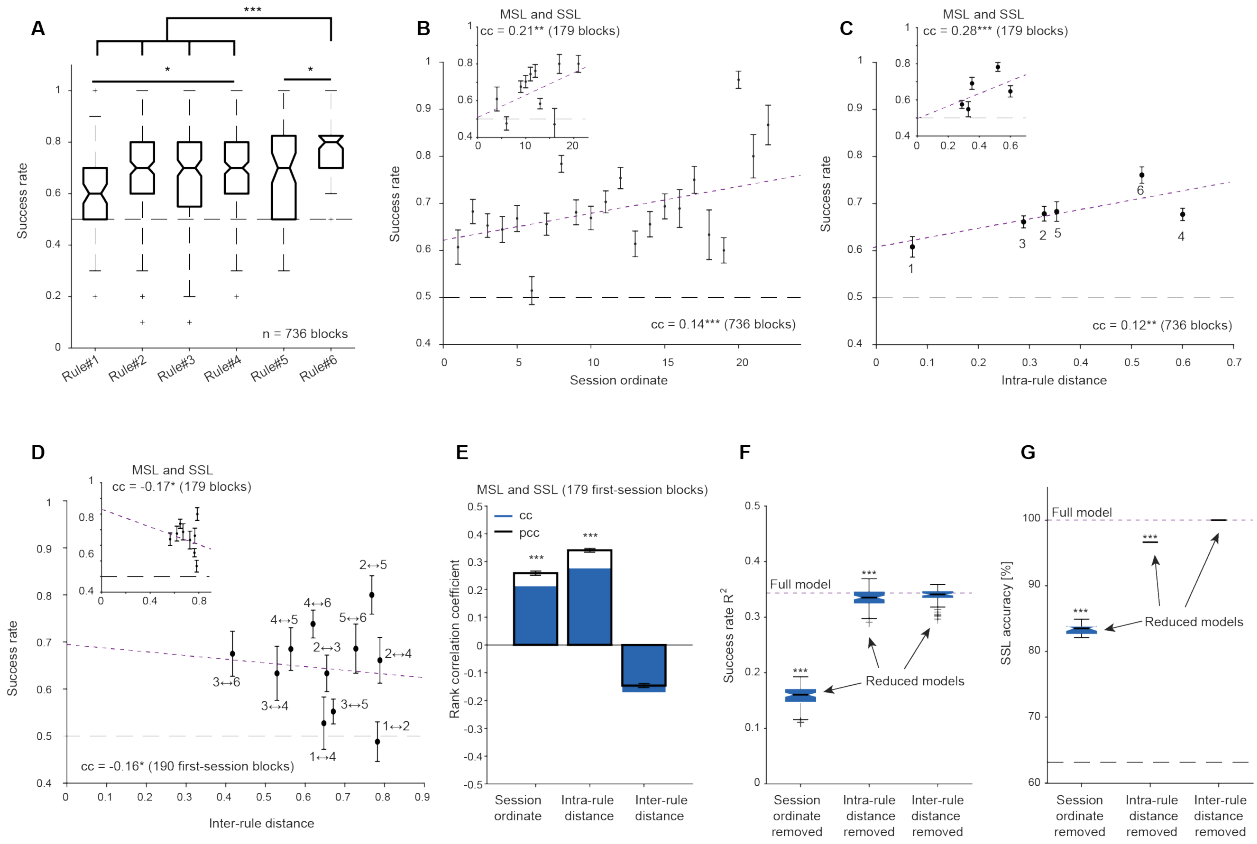

Figure 3. Single session learning can be predicted based on experience and rule difficulty. (**A**) Success rates for individual rules. */***: p<0.05/p<0.001, Kruskal-Wallis test, corrected for multiple comparisons. (**B**) Success rates vs. animal experience, quantified by the session ordinate. Here and in **C** and **D**, purple lines represent linear model fit. **Inset**, Success rate vs. session ordinate for a reduced set of SSL and MSL sessions. Here and in **C**, **D** and **E**, */**/***: p<0.05/p<0.01/p<0.001, permutation test. (**C**) Success rates vs. rule difficulty, quantified by the intra-rule distance metric (**Fig. 1D**). (**D**) Success rates vs. the similarity between the new and the previous rule. Only first post-transition sessions are included. (**E**) Rank correlation coefficients (cc) and partial rank correlation coefficients (pcc) between success rate and the features described in **B**-**D**. (**F**) Variance in block success rate (R^2) explained by cross-validated support vector regression models. ***: p<0.001, Bonferroni-corrected U-test between the R^2 of the full model and the R^2 of the reduced model obtained after removing one feature. (**G**) Accuracy in predicting SSL using cross-validated support vector classification. ***: p<0.001, Bonferroni-corrected U-test between the accuracy of the full and reduced models.

To determine the total variability of success rate explained by the three features, we used support vector regression. Over a third of the variability in block success rate was explained (R^2=0.34 [0.33 0.35]; median [IQR] of n=20 independent ten-fold cross-validated models; **Fig. 3F**). By excluding one feature at a time, we found that experience made a dominant contribution to success rate (R^2=0.16; p<0.001, U-test corrected for multiple comparisons; **Fig. 3F**). Intra-rule distance also made a consistent contribution (R^2=0.33; p<0.001), whereas inter-rule distance did not (R^2=0.34, p=0.06). Thus, the most important feature in determining success rate during the first session of a new rule is experience.

Knowing that success rate in the first session of a newly encountered rule depends on mouse experience and rule difficulty, we assessed what determines SSL. We used cross-validated binary classification (support vector machines) to predict whether a given first session block is SSL or MSL. The prediction of SSL from animal experience and physical rule properties was perfect (100% accuracy; **Fig. 3G**). By excluding one feature at a time, we found that prediction depended on experience (83% [83% 84%]; p<0.001; **Fig. 3G**) and intra-rule distance (97% [97% 97%]; p<0.001). Prediction did not depend on inter-rule distance (p=1). Thus, knowing how experienced the animal is and what are the physical properties of a new rule allows predicting whether SSL will occur.

When conditions are favorable, mice can generalize from similar yet easier rules

The negligible reduction in variability explained by inter-rule similarity during SSL and MSL sessions (**Fig. 3F**) suggests that mouse strategy during learning the set of arbitrary rules was not based on generalization. Minimizing the usage of generalization may be specific to the set of arbitrarily rules, for which median [IQR] inter-rule distances were 0.65 [0.53 0.77] (n=11 transitions; **Fig. 3E**). To determine whether mice employ a different strategy when consecutive rules are similar, we tested two subjects on a set of five new rules (m5 and m6; **Fig. 4**). The first new rule was easiest, followed by gradually more difficult rules (**Fig. 4A**). All inter-rule distances between consecutively-presented rules were 0.04. After reaching stable performance on the first new rule (#7), every rule was presented for one session. Despite the increasing difficulty, both mice achieved SSL for rules #8-10 (**Fig. 4B**). For instance, intra-rule distances of rule#8 and rule#9 were 0.2 and 0.12 (**Fig. 4A**), more difficult than rules #2-6 that were associated with SSL (range: [0.29,0.6]; **Fig. 1D**). Nevertheless, SSL was readily achieved for rules #8-10. Even the most difficult rule (#11; intra-rule distance, 0.04) was associated with SSL in one subject (m6; **Fig. 4B**). Thus, when inter-rule similarity is high, SSL can be achieved for difficult rules.

The new rules #7-11 were presented at the same order to both mice. However, success rates during rules #8-10 were not consistently lower than during rule#7 (p=1, p=0.86, and p=0.85, Kruskal-Wallis test; **Fig. 4C**). In contrast, success rates during rule#11 were lower than during rule#10 (p=0.02), although inter-rule distance between rule#10 and rule#11 was identical to the distance between every other pair of consecutively-presented rules. Success rates were correlated with intra-rule distance (cc: 0.42; n=83 blocks; p<0.001, permutation test; **Fig. 4D**). However, the distances of the points representing rules #7-10 from the linear model fit to the arbitrary rules (**Fig. 4D**, purple line) were higher than for rules #1-6 (p=0.013, p=0.0013, p=0.0013, and p=0.0004, U-test; **Fig. 4D**). In contrast, rule#11 did not deviate from the line (p=1), suggesting that under the conditions of the task, rule#11 was close to the "just noticeable difference" of visual discrimination. Regardless, success rates of rules #7-10 are higher than expected given the difficulty of the rules and the pattern established by the arbitrary rules.

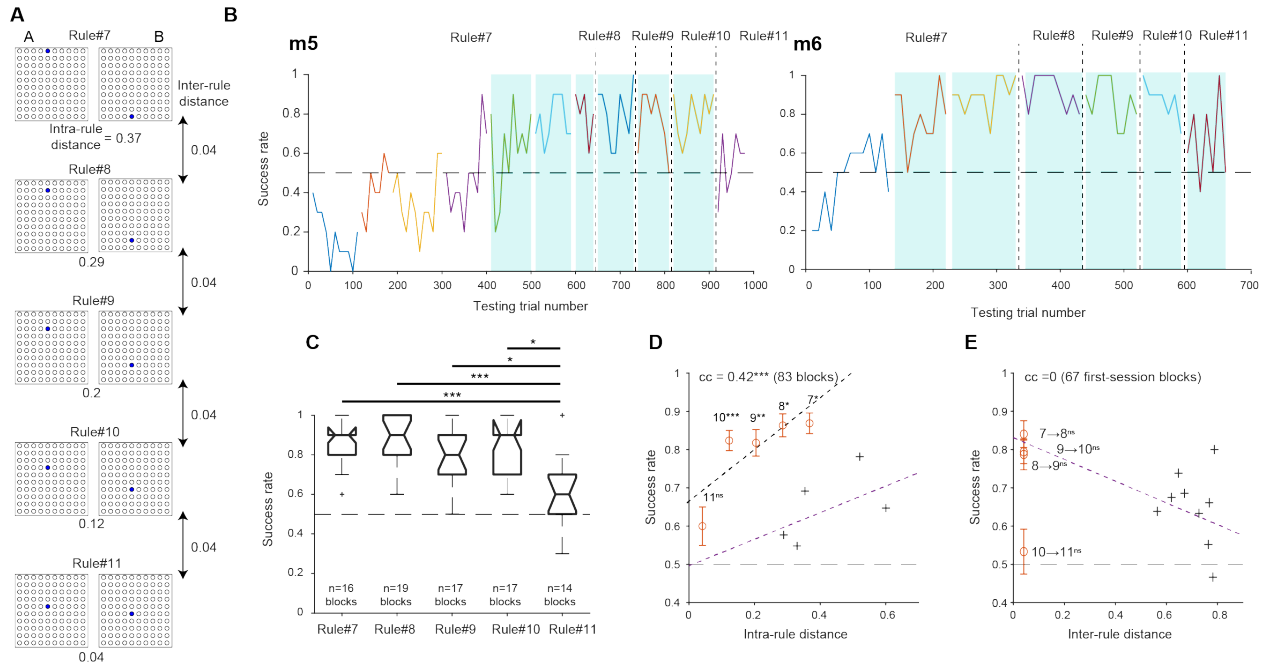

Figure 4. When conditions are favorable, mice can generalize from similar yet easier rules. (**A**) Five visual rules of increasing difficulty, distinct from rules #1-6 (**Fig. 1D**). (**B**) Success rates as a function of testing trial number. After performance on rule#7 stabilized, a new rule of higher difficulty was employed on every session. All conventions are the same as in **Fig. 2A**. (**C**) Success rates for individual rules. Here and in **D-E**, only the last session of rule#7 was used. */***: p<0.05/p<0.001, U-test. (**D**) Success rates vs. rule difficulty. ***: p<0.001, permutation test. Here and in **E**, crosses and purple lines represent data points and linear models copied from **Fig. 3C** (and **Fig. 3D**) **inset**. Here and in **E**, ns/*/**/***: p>0.05/p<0.05/p<0.01/p<0.001, U-test. (**E**) Success rates vs. the similarity between the new and the previous rule.

The higher-than-expected success rate of rules #8-10 may be explained by generalization from similar yet easier rules. Since all inter-rule distances were identical (0.04), success rates could not be directly correlated with inter-rule distances (**Fig. 4E**). The distances of rules #8-11 from the linear fit to the arbitrary rules were not consistently different than for rules #1-6 (p=0.6, p=0.62, p=0.11, and p=0.056, U-test; **Fig. 4E**). Thus, SSL of particularly difficult rules can be facilitated by generalization from similar yet easier rules. Indeed, success rates during SSL sessions with low inter-rule distances (rules #7-11; 0.85 [0.7 0.9]; n=67 blocks) were consistently higher than for high inter-rule distances (rules #1-6; 0.7 [0.6 0.8], n=112; p=0.0002, U-test). In sum, when conditions for generalization are more favorable, mice perform SSL with higher success rate.

Units recorded during the visual task exhibit place fields and state-dependent modulation

To determine how neuronal activity is modulated while performing a previously-learned rule, we implanted m4 with a high-density probe in CA1. After recovery from surgery, the mouse was retrained on rule#2 and multi-neuronal activity was recorded from str. radiatum during three consecutive sessions (**Fig. 5A**). An example unit spiked at different locations along the central arm of the T-maze (**Fig. 5B**). Although the mouse spent most of the time near the reward ports (**Fig. 5C, left**), firing rate was consistently high at two other regions (p<0.001, Bonferroni-corrected Poisson test comparing to the mean rate; **Fig. 5C, center**). Thus, the example unit exhibited two place fields on the central arm (**Fig. 5C, right**). 21/84 (25%) of the active units had at least one place field (p<0.001, Binomial test; **Fig. 5D, left**), some exhibiting two or three fields (**Fig. 5D, right**). The 31 place fields were scattered all over the T-maze (**Fig. 5E, left**). However, the fraction of fields with centers in regions where a stimulus was available (home box and central arm) was consistently above chance (area-based chance level, 50%; p=0.002, Binomial test; occupancy-based chance level, 17%; p<0.001; **Fig. 5E, right**). Thus, place fields are found predominantly at locations related to the stimulus and choice, rather than the reward.

Task-related neuronal activity may manifest as state-dependent firing rate modulation. An example unit showed selectivity towards right-going as opposed to left-going trials (**Fig. 5F**). Here, the absolute difference in firing rate between right and left trials at the location of the maximal joint firing rate was consistently above chance (p=0.03; permutation test; **Fig. 5F**). Another unit exhibited higher firing rates during testing compared with training trials (p=0.008; **Fig. 5G**). Selectivity towards testing trials appeared when the animal approached the choice point (**Fig. 5G**). Overall, 9/84 (11%) units exhibited right/left firing rate modulation (p=0.03, Binomial test; **Fig. 5H**), and 19/84 (26%) units exhibited training/testing modulation (p<0.001). Thus, task-related information is differentially represented in single-unit activity.

A mouse trained on the visual task can learn an intra-cortical rule

Ultimately, discrimination between sensory stimuli converges to differentiating between neuronal activity patterns. To determine whether freely-moving mice are capable of successive conditional discrimination learning of intra-cortical rules, we implanted m1 with six LED-coupled optical fibers and activated CA1 pyramidal cell dendrites in str. radiatum (**Fig. 6A, top**). Two intra-cortical rules were used (**Fig. 6A, bottom**). Rule#12, {A: LEDs #1-2 flickering at 4 Hz, 20% duty cycle; B: LEDs #5-6 flickering at 10 Hz, 50% duty cycle}, had an intra-rule distance of 0.51. For rule#13, {A: all LEDs off; B: LEDs #1-6 flickering at 40 Hz, 50% duty cycle}, the intra-rule distance was 0.79.

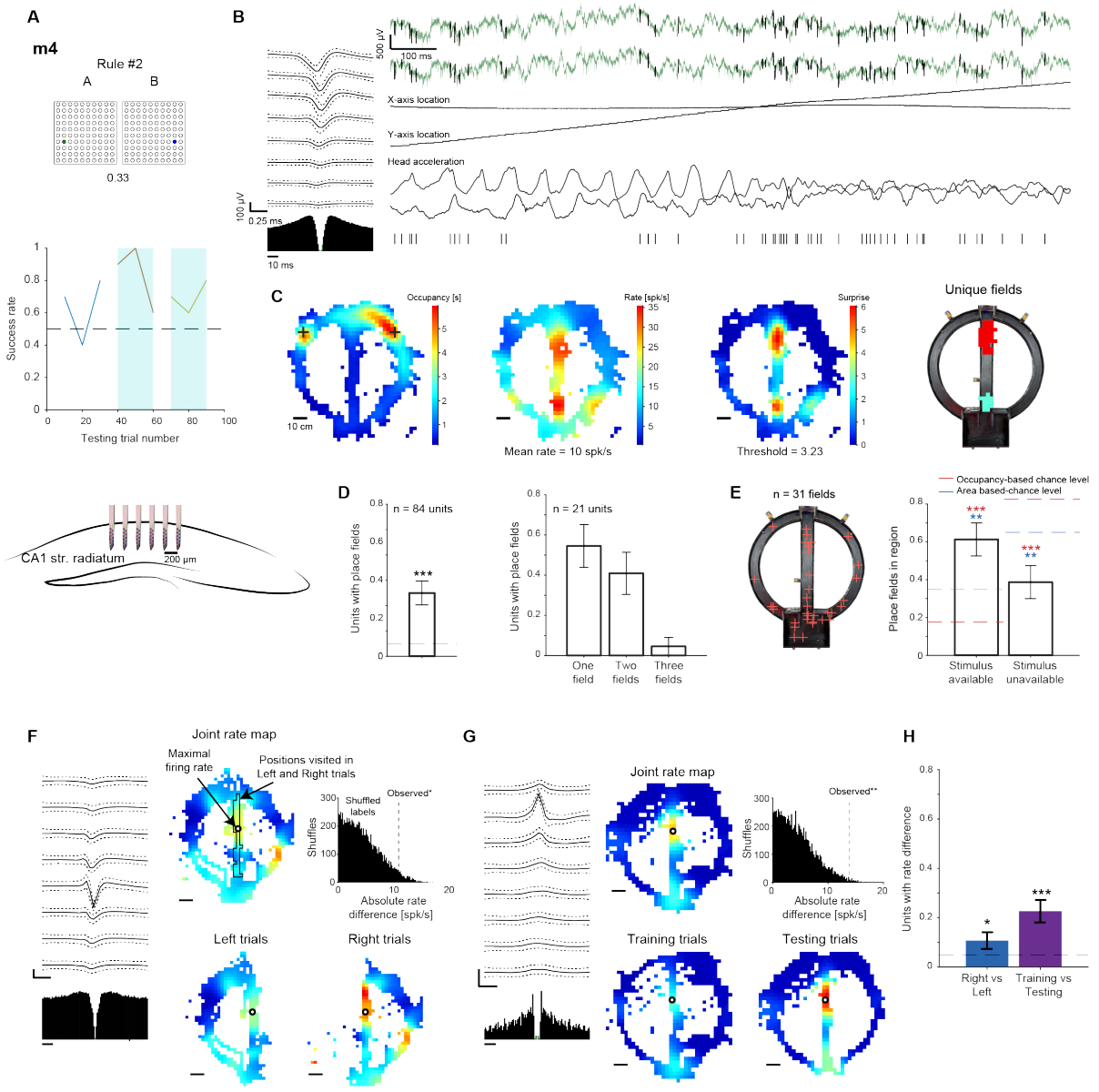

Figure 5. Units recorded during the visual task exhibit place fields and state-dependent modulation. (**A**) Subject m4 was implanted with a high-density probe in CA1 and retrained on rule#2.(**B**) Example unit. **Top left**, Mean waveform. **Bottom left**, Autocorrelation histogram. **Top right**, Wide-band (0.1-7,500 Hz) traces recorded by two adjacent electrodes during a single run along the central arm. **Center right**, Animal kinematics. **Bottom right**, Spike times. (**C**) The unit exhibits two place fields. **Left**, Occupancy map, quantifying the time spent at every position during all training and successful testing trials. Plus signs, reward ports. **Center left**, Rate map. **Center right**, Surprise, negative base-10 logarithm of the probability to obtain the observed number of spikes or more. **Right**, Both place fields are on the central arm. (**D**) Fraction of units with place fields, and number of place fields per unit. Here and in **E** and **H**, */**/***: p<0.01/p<0.05/p<0.001, Binomial test. (**E**) **Left**, Locations of place fields centers. **Right**, Fraction of place fields in regions where a stimulus is available. (**F**) Example unit exhibiting higher firing rate during right-choice compared with left-choice trials. **Top center**, Rate map. **Bottom**, Separate right/left rate maps. **Top right**, Dashed line, absolute firing rate difference between left and right trials at the point of maximal joint firing rate. Here and in **G**, */**: p<0.05/p<0.01, permutation test. (**G**) Example unit exhibiting higher firing rate during testing compared with training trials. (**H**) The fraction of units with left/right modulation or with train/test modulation. Dashed line, chance level.

Over two sessions, the mouse did not learn rule#12, showing no improvement between blocks (cc: 0.19; n=20 blocks; p=0.42, permutation test; **Fig. 6B**). In contrast, the mouse achieved MSL on rule#13 and performed the task correctly during two consecutive sessions (p=0.003 for each session, Binomial test; **Fig. 6B**). Success rate on rule#13 was 0.6 (n=52 blocks), not consistently different from MSL success rates on rules #1-6 (p=0.89, U-test; **Fig. 6C**). Success rates of rules #12-13 were lower than expected based on rule difficulty (rule#12: p=0.03; rule#13: p<0.001, U-test; **Fig. 6D**), suggesting that intra-cortical rules were more difficult to learn compared with the arbitrary visual rules. The inter-rule distance between rule#12 and rule#13 was 0.65, in the regime where conditions for generalization are not favorable. Nevertheless, rule#13 success rate was in agreement with the relation between inter-rule distance and success rate observed for the arbitrary rules (p=0.76; **Fig. 6E**), Thus, a mouse previously trained on visual rules can perform MSL on intra-cortical rules.

Discussion

We tested the ability of mice to quickly learn new rules that span a range of difficulties. After acquiring the basic paradigm, subjects can learn a new visual rule within a single session. Remarkably, all animals achieve SSL of at least one rule. When SSL occurs, mice successfully perform the task from the first block. SSL is achieved when experienced mice engage in a relatively easy rule or can generalize from previously learned rule.

Rule learning as part of multilevel learning

Rule learning in a discrimination task with changing rules requires four levels of learning. The first is a type of procedural learning, in which the general task logic is acquired. In the present 2AFC paradigm, the logic involves learning that certain running directions are permitted, that doors open and close, that water are available at two specific locations, and so on. The logic is learned during the shaping period and is independent of the existence of a discrimination rule.

The second level involves learning that there is a stimulus-response contingency. Here, the animal learns that during testing trials, water is available only if the response to the stimulus is correct. The first two levels of learning generate the long-term memory component of standard successive conditional discrimination tasks[24]. When shaping is conducted prior to training on a specific stimulus-response contingency, the two levels may be separated[10,34]. Then, performance is tested on the second level, as done in the present experiments with the first rule presented to every mouse.

The third level of learning is learning how to learn. Learning that the rules of the task can change between sessions is a long-term memory component that improves with experience, independent of the other two levels of learning. When the rule is fixed during all sessions, the subject may still improve between sessions. Only when the rules change, the ability of learning to learn a new rule can be assessed.

The fourth and final level arises after behavior becomes procedure[2,3] and involves learning a specific new rule in a well-known setting. Successful performance may be achieved via associative learning of the new rule, via generalization or transfer from a similar rule, or by applying a familiar rule to a new set of cues (categorization). By definition, learning a new rule during a single session requires reference memory[30-33]. Unless a new rule is introduced, behavior gradually becomes procedural[5] and the fourth level cannot be assessed. Moreover, associative learning cannot be guaranteed if the new rule can be

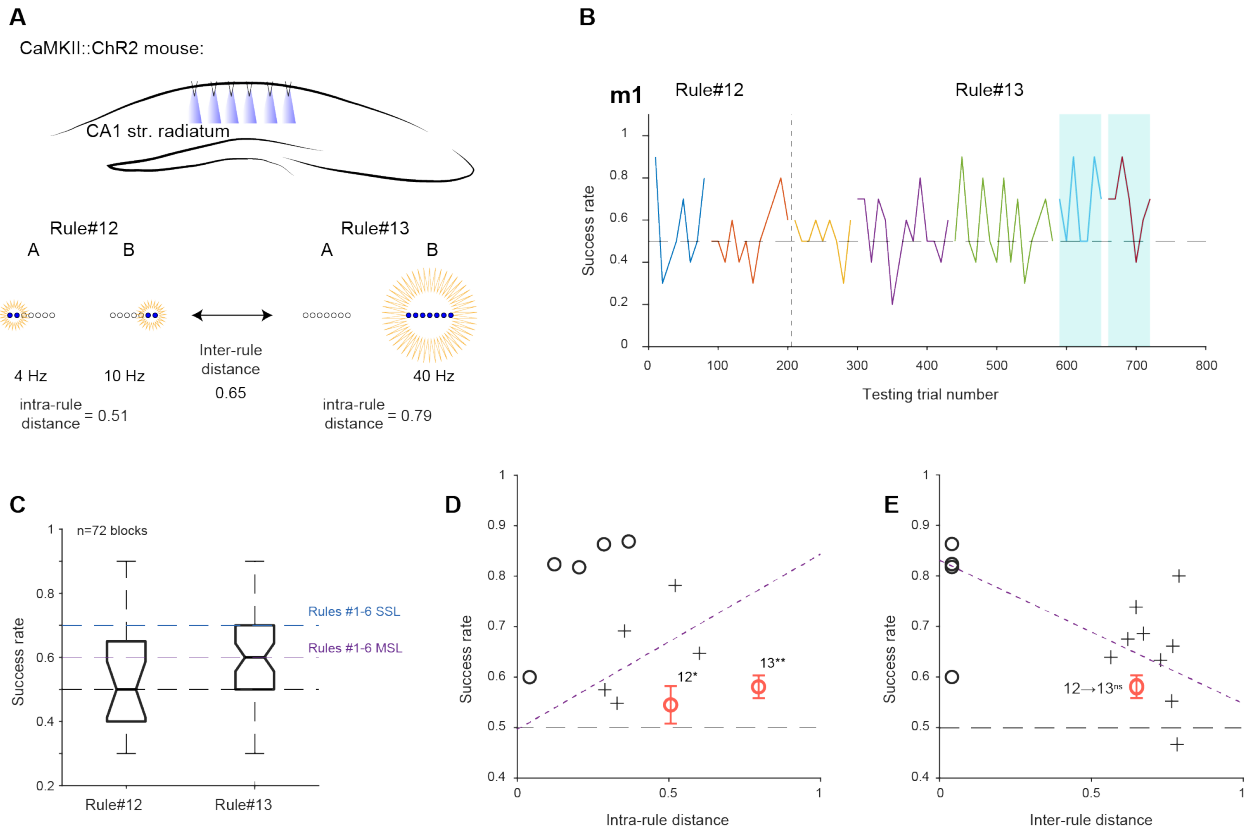

Figure 6. A mouse trained on the visual task can learn an intra-cortical rule. (**A**) Instead of using visual stimuli, the task was governed by intra-cortical stimuli applied to pyramidal cell dendrites via six optical fibers implanted in CA1 str. radiatum of a CaMKII::ChR2 mouse. (**B**) Success rate as a function of testing trial number. All conventions are the same as in **Fig. 2A**. (**C**) Success rates during intra-cortical rules. Purple and blue lines represent median success rates of all visual MSL and SSL success rates (**Fig. 2F**). (**D**) Success rates vs. rule difficulty. Crosses and dashed purple line represent data points and linear model copied from **Fig. 3C**; black circles are copied from **Fig. 4D**. Here and in **E**, ns/*/**: p>0.05/p<0.05/p<0.01, U-test. (**E**) Success rates vs. the similarity between the new and the previous rule. Crosses and dashed purple line represent data points and linear model copied from **Fig. 3D**; black circles are copied from **Fig. 4E**.

categorized by, or generalized from, previously learned rules.

Tasks that involve generalization[7,35,36], transfer[8,9], or categorization[10,35,37] involve the first two levels but do not require associative learning. The finding that a new rule can be learned during the very first block indicates that mice can learn to discriminate from a small number of samples, emphasizing the importance of reference memory when conditions in a familiar environment change. Previous work showed that rodents can learn from a few samples in the Morris water maze[19,20], fear conditioning[15,16], or labyrinth navigation[17]. Yet in all aforementioned studies, only two levels of learning were tested. In the radial arm maze[30], the specific set of arms baited during the session allows to also test the fourth level (reference memory). However, the rule governing the task remains unchanged. Thus, the process of "learning to learn" was not assessed by previous work.

The finding that experience is crucial for SSL becomes clear considering the multilevel learning framework suggested here. The "learning to learn" process implies that a more experienced animal is more flexible to changes in the environment and more likely to learn a new rule quickly. Nevertheless, learning a rule during SSL is limited to a single session. Thus, learning a specific new rule (the fourth level) is a process distinct from all processes that depend on long-term memory. The fact that easier rules are more likely to be learned supports the multilevel framework.

Generalization

Other cognitive processes may be utilized when two consecutive rules are similar. Learning a new rule when the conditions for generalization are favorable is not independent of the past. Previous work found that rats can use transfer learning to perform a difficult discrimination task[8]. Rodents also excel in categorized learning[10,38,39]. In both cases, the animal generalizes from previously learned rules and can solve the task without learning new associations as in the fourth level of learning suggested above. Indeed, when inter-rule distances were lower, success rates were higher (**Fig. 4E**). Furthermore, SSL was achieved even for difficult new rules, suggesting that mice did not necessarily learn the new rule, which would have required associative learning and reference memory. Instead, the animals may have categorized the cues comprising the new rule using previously acquired knowledge.

Limitations

While intra-rule distances spanned the entire range of possible values, inter-rule distances were sampled only for high (>0.4) or very low (0.04) values. When encountering intermediate inter-rule distances mice may exhibit different strategies, or change strategy according to the relation between intra- and inter-rule distances.

Given single-block learning, the fifteen-trial block size employed yields an upper bound on the number of trials required to learn a new rule. Smaller blocks may yield improved estimates of the minimal number of trials required for mice to carry out successful operant learning of a new rule.

Neuronal mechanisms underlying rule learning

Due to high reproductive rate, genetic control, and well-established tasks for a plethora of behaviors, mice have emerged as a robust model for studying various neuronal mechanisms[40-44]. Head-fixed and freely-moving mice allow combining behavioral and neuronal recordings[24,26] and manipulations[45]. Extensive correlative evidence links neuronal activity with learning, perception, and discrimination[46-48].

Indeed, neuronal mechanisms underlying operant learning are often studied using rodents performing a sensory discrimination task[26,49-52]. Learning across multiple sessions limits the interpretational power yielded by most rodent learning tasks. SSL can increase the overlap between the recorded neuronal activity and the act of learning. To our knowledge, the cellular-network mechanisms underlying the process of rapid successive conditional discrimination learning requiring the use of reference memory are unknown. We showed that the activity of hippocampal neurons is modulated by the task and conversely, that optogenetic manipulations can generate behavioral responses. It remains for future work to determine the neuronal mechanisms underlying learning to learn.

Acknowledgements

We thank Ortal Amber-Vitos, Amir Globerson, and Shirly Someck for discussions, Yuval Te'eni for help training animals, and Lirit Levi, Shir Mendelbaum, and Hadas Sloin for constructive comments. This work was supported by the United States-Israel Binational Science Foundation (BSF; 2015577); by European Research Council 679253; by the Israel Science Foundation FIRST Program (1871/17); by the Canadian Institutes of Health Research (CIHR), the International Development Research Centre (IDRC), the Israel Science Foundation (ISF), and the Azrieli Foundation (2558/18); and by the Zimin Institute.

Author contributions

A.L. and E.S. conceived and designed the experiments, implanted animals, analyzed data, and wrote the manuscript. A.L. built the experimental apparatus. A.L. and N.A. carried out experiments.

Declaration of interests

The authors have declared that no competing interests exist.

Materials and Methods

Experimental animals

A total of six adult hybrid mice, one male and five females, were used in this study (**Table 1**). Hybrid mice were used since compared to the progenitors, hybrids exhibit reduced anxiety-like behavior, improved learning, and enhanced running behavior[21]. Four of the mice (m1-m4) were hybrid and double-transgenic, the F1 generation of an FVB/NJ female (JAX #001800, The Jackson Labs) and a male offspring of an Ai32 female (JAX #012569) and a CaMKII-Cre male (JAX #005359). The other two mice (m5 and m6) were offspring of an FVB/NJ female and a PV-Cre male (JAX #008069). After separation from the parents, animals were housed in groups of same-litter siblings until participation in experiments. Animals were held on a reverse dark/light cycle (dark phase, from 8 AM until 8 PM). All animal handling procedures were in accordance with Directive 2010/63/EU of the European Parliament, complied with Israeli Animal Welfare Law (1994), and approved by the Tel Aviv University Institutional Animal Care and Use Committee (IACUC #01-16-051 and #01-21-061).

Water deprivation

Mice were trained on a two-alternative forced-choice (2AFC) task in which the rules governing discrimination behavior could change between different sessions. Every session was conducted on a different day. At the beginning of the training period, animals were housed one per cage and placed on a water-restriction schedule that guaranteed at least 40 ml/kg of water every day, corresponding to 1 ml for a 25 g mouse. Training was carried out five days a week, and animals received free water on the sixth day. Reward volume differed between mice and sessions, ranging 4-20 µl. The exact volume was determined by the experimenter before each session based on familiarity with the specific animal. In all sessions, the reward was larger by 20-50% during testing compared with training trials.

Apparatus

The apparatus was a circular T-maze equipped with five motorized doors, five photosensors, two solenoid-driven reward ports, and a 100-LED visual stimulation matrix (**Fig. 1A**). All sensors and actuators were controlled by a microcontroller (Arduino Mega) via custom designed electronic circuitry. The home box (L x W x H: 20 x 30 x 10 cm) was located at the beginning of the central arm (75 x 8 x 3 cm) and connected to the end of the two lateral arms (100 x 6 x 3 cm). Each passageway between the home box and one of the arms was blocked by a transparent polycarbonate door. Two additional doors were located at the sides of the T-junction at the end of the central arm, blocking passage to the lateral arms. Every door was operated by a small motor (DC 6V 30RPM Gear Motor, Uxcell) and was equipped with two limit switches (D2F-01L2, Omron). There were five photosensors (PS; S51-PA-2-A00-NK, Datasensor). Water rewards were given by solenoids (003-0137-900, Parker), and each water port was connected to a different solenoid via flexible (Tygon) tubing. The visual stimulation matrix was constructed of 10 x 10 LEDs in alternating columns of blue (470 nm, Cree) and green (527 nm, Cree) diodes.

Discrimination task

On a given session, a single rule consisting of two cues was used. Cue A was associated with leftward runs, and cue B was associated with rightward runs. Allocation of cues A and B to trials was pseudo-

random. The {A; B} pair of cues could correspond to one of two modalities, visual or intra-cortical. There were two types of sessions, "shaping" (pretraining) and "learning". Shaping sessions included only "training" trials. Initially, each mouse was acquainted with the task in a series of shaping sessions (median [range]: 5 [4,10] sessions). Mice had to reach a criterion of 50 trials per session before commencing learning sessions. On each session, mice were free to perform the task until losing interest. Loss of interest was identified by behavior that included prolonged periods of rest and attempts to climb the walls of the home box. Learning sessions were divided into blocks, and every block included five training trials and ten "testing" trials.

A single "testing" trial proceeded as follows: (1) *Stimulus*: Once the animal entered the home box and passed the photosensors, the entrance doors (D4 and D5) closed and the exit door (D1) to the central arm opened (**Fig. 1A**). At the same time, a cue A or B was given. (2) *Run*: Once the animal left the home box and passed the central arm photosensor, the two lateral doors (D3 and D4) at the T-junction opened, and the exit door (D1) closed. During the Run, the stimulus was continuously available. (3) *Response*: The animal chose a direction at the T-junction and went through one of the two open doors. Once the animal passed the lateral arm photosensor, the stimulus turned off and the doors closed. (4) *Reward*: A liquid reward was available at the corresponding water port if the animal made a correct choice. The animal could not go back to the T-junction, but was free to consume the reward and return to the home box through the open home box door (D4 or D5).

During "training" trials, only the corresponding door (D3 or D4) at the T-junction opened. Because the animal could make an incorrect choice, a reward was given during every training trial.

Probes and surgery

Two of the mice (m1 and m4) were used for electrophysiological recordings and optogenetic manipulations. The animals were implanted with a multi-shank silicon probe attached to a movable micro-drive, equipped with optical fibers following previously described procedures[53]. The probes used were Stark64 (Diagnostic Biochips), consisting of six shanks, spaced horizontally 200 μm apart, with each shank consisting of 10-11 recording sites spaced vertically 15 μm apart (micrograph in **Fig. 5A**). Probes were implanted in the parietal neocortex above the right hippocampus (AP/ML, 1.6/1.1 mm; 45° angle to the midline) under isoflurane (1%) anesthesia.

Recordings and spike sorting

Implanted animals were equipped with a three-axis accelerometer (ADXL-335, Analog Devices) for monitoring head movements. Head position and orientation were tracked in real-time using two head-mounted LEDs, a machine vision camera (ace 1300-1200uc, Basler), and a dedicated system[54]. During every recording session, baseline neural activity was recorded for at least 15 min while the animal was in the home cage. During some sessions, the animal was then placed on the apparatus, followed by additional recordings in the home cage. After every session, the probe was translated vertically downwards by up to 70 μm.

Neural activity was filtered, amplified, multiplexed, and digitized on the headstage (0.1–7500 Hz, x192; 16 bits, 20 kHz; RHD2164, Intan Technologies) and then recorded by an RHD2000 evaluation board (Intan Technologies). Offline, spikes were automatically detected and sorted into single units using

KlustaKwik3[55]. Automatic spike sorting was followed by manual adjustment of the clusters. Only well-isolated units were used for further analyses (amplitude >40 μV; L-ratio <0.05; ISI index <0.2[40]).

Quantification of rule difficulty and inter-rule similarity

To place arbitrary rules on a continuous scale, a symmetric intra-rule distance metric was introduced (e.g., **Fig. 1D**). To derive the metric, every rule was characterized by three physical attributes that quantified the difference between the cues A and B. (1) The correlation distance (cd): One minus the maximal value of the 2D cross-correlation coefficient between A and B. (2) The Euclidean distance (ed): The scaled distance between the optimal match that yields the correlation distance. (3) The luminance distance (ld): The scaled difference in luminance between A and B. All distances (cd, ed, and ld) are non-negative scalars limited to the [0,1] range. The distance metric is then the magnitude of the 3D vector, defined as

$$d_{intra} = d_{AB} = \sqrt{\frac{cd(A,B)^2+ed(A,B)^2+ld(A,B)^2}{3}}.$$

The metric ranges [0,1], taking the value of 0 when the two cues are identical (impossibly-difficult rule) and 1 when cues are maximally distinct (very easy rule).

The same physical attributes that characterize each rule were used to measure the difference between distinct rules (e.g., **Fig. 3D**). The inter-rule distance is a symmetric measure of the difference between the physical properties of the same-laterality cues of the two rules. Thus, for a pair of rules {A; B} and {A'; B'}, the inter-rule distance is the average of the intra-rule distances for two "mixed" rules: {A; A'} and {B; B'}. The resulting metric is

$$d_{inter} = (d_{AA'} + d_{BB'})/2.$$

The metric takes the value of 0 when the two rules are identical and 1 when the rules are maximally distinct.

Trial-averaged rate maps

To create trial-averaged firing rate maps (**Fig. 6**), we first defined a trial as a single run starting and ending at the home box photosensors. Time segments that occurred while the speed of the animal was below 5 cm/s were omitted. The spikes in every trial were binned into 2.5 x 2.5 cm bins. Then, count and temporal occupancy maps were constructed and smoothed with a 2D Gaussian kernel that had an SD of 5 cm. A firing rate map was computed for each trial by dividing every bin in the smoothed count map by the corresponding bin in the smoothed occupancy map. For every unit, five trial-averaged rate maps were constructed by calculating the mean firing rate in every spatial bin, weighted by the value in the corresponding bin of the occupancy map. (1) Joint rate map, based on all training trials and all correctly-performed testing trials. (2) Correct left trials, based on all trials in which the correct choice was "go-left". (3) Correct right trials. (4) Training trials. (5) Correct testing trials. A total of 84/92 units (91%) fired one or more spikes on the arena and were used for analysis.

Identification of place fields

To detect place fields in a rigorous statistical manner, we extended the Poisson method for field detection on the linear track[42] to 2D. Formally, place fields were defined as contiguous regions in which the firing rate deviated from chance, evaluated as follows. First, the mean firing rate λ was computed by an occupancy-weighted average of the entire rate map. Second, the Poisson probability to obtain the observed (or higher) number of spikes in the bin, given the time spent in the bin and λ, was estimated. Third, the number of effectively independent bins was determined by the full-width at half-height of the 2D autocorrelation of the rate map. The probability in every bin was compared to the Bonferroni-corrected chance level. Finally, a place field was defined as a contiguous set of bins with above-chance firing rates. Overall, 31 place fields were identified in 84 units.

State dependent modulation of firing rate

To determine whether the firing rate of a given unit differed in two conditions (e.g., left vs. right trials; training vs. testing trials), we used a permutation test. First, we determined a region of interest (ROI) on the maze by identifying the single bin in the joint rate map with the maximal firing rate. In the case of two conditions with different occupancy maps (e.g., right and left trials), the ROI was constrained to be in the overlapping region. Second, we computed a statistic, the absolute firing rate difference between the two condition-specific rate maps at the ROI. Third, we shuffled the labels of the trials (10,000 times), recomputed the condition-specific rate maps, and recomputed the statistic. The null hypothesis is that the absolute firing rate difference do depend on the labels. Finally, the probability of accepting the null was estimated by the number of cases in which the shuffled firing rate difference was higher than the observed firing rate difference.

Statistical analyses

In all statistical tests used in this study, a significance threshold of α=0.05 was used. All descriptive statistics (n, median, IQR, range) can be found in the Results, figures, and figure legends. All analyses were conducted in MATLAB (MathWorks). Nonparametric statistical tests were used throughout. Differences between medians of two groups were tested with Mann-Whitney's U-test (two tailed). Differences between medians of three or more groups were tested with Kruskal-Wallis nonparametric analysis of variance and corrected for multiple comparisons using Tukey's procedure. Wilcoxon's signed-rank test was employed to determine whether a group median is distinct from zero (two tailed). To estimate whether a given fraction was smaller or larger than expected by chance, an exact Binomial test was used. A permutation test was used to estimate significance of rank correlation coefficients.

Tables

Table 1. List of experimental animals

No.	Animal ID	Sex	Strain[1]	Paternal strain[2]	Age[3] [week]	Weight[3] [g]	Probe
m1	mC41	Male	HYB	CaMKII::Ai32	26	39.4	Stark64
m2	mA154	Female	HYB	CaMKII::Ai32	14	26.5	
m3	mA350	Female	HYB	CaMKII::Ai32	13	15.7	
m4	mA354	Female	HYB	CaMKII::Ai32	13	16.4	Stark64
m5	mE177	Female	HYB	PV-Cre	21	22.4	
m6	mE178	Female	HYB	PV-Cre	21	26.3	

[1]All mice were hybrid (HYB), the F1 offspring of an FVB/NJ female (JAX #001800) and a C57-derived male.

[2]The paternal strain was either an offspring of an Ai32 female (JAX #012569) and a CaMKII-Cre male (JAX #005359); or a PV-Cre male (JAX #008069).

[3]At the beginning of training.

References

1. Thorndike, E. L. The law of effect. Am. J. Psychol. *39*, 212–222 (1927).
2. Kandel, E.R., Schwartz, J.H., Jessell, T.M., Siegelbaum, S., Hudspeth, A.J., and Mack, S. (2000). Principles of neural science (McGraw-hill New York).
3. Simor, P., Zavecz, Z., Horváth, K., élteto, N., Török, C., Pesthy, O., Gombos, F., Janacsek, K., and Nemeth, D. (2019). Deconstructing procedural memory: Different learning trajectories and consolidation of sequence and statistical learning. Front. Psychol. *9*, 2708.
4. Tricomi, E., Balleine, B.W., and O'Doherty, J.P. (2009). A specific role for posterior dorsolateral striatum in human habit learning. Eur. J. Neurosci. *29*, 2225–2232.
5. Gillan, C.M., Otto, A.R., Phelps, E.A., and Daw, N.D. (2015). Model-based learning protects against forming habits. Cogn. Affect. Behav. Neurosci. *15*, 523–536.
6. Carey, S., and Bartlett, E. (1978). Acquiring a single new word. Papers and Reports on Child Language Development. *15*, 17-29.
7. Samborska, V., Butler, J.L., Walton, M.E., Behrens, T.E.J., and Akam, T. (2022). Complementary task representations in hippocampus and prefrontal cortex for generalizing the structure of problems. Nat. Neurosci. 25, 1314–1326.
8. Murphy, R.A., Mondragón, E., and Murphy, V.A. (2008). Rule learning by rats. Science *319*, 1849–1851.
9. Kurt, S., and Ehret, G. (2010). Auditory discrimination learning and knowledge transfer in mice depends on task difficulty Proc. Natl. Acad. Sci. USA. *107*, 8481–8485.
10. Broschard, M.B., Kim, J., Love, B.C., and Freeman, J.H. (2021). Category learning in rodents using touchscreen-based tasks. Genes. Brain. Behav. *20*, e12665.
11. Reinert, S., Hübener, M., Bonhoeffer, T., and Goltstein, P.M. (2021). Mouse prefrontal cortex represents learned rules for categorization. Nature *593*, 411–417.
12. Higgins, G.A., Grzelak, M.E., Pond, A.J., Cohen-Williams, M.E., Hodgson, R.A., and Varty, G.B. (2007). The effect of caffeine to increase reaction time in the rat during a test of attention is mediated through antagonism of adenosine A2A receptors. Behav. Brain Res. *185*, 32–42.
13. Chun, M.M., and Jiang, Y. (1998). Contextual cueing: Implicit learning and memory of visual context guides spatial attention. Cogn. Psychol. *36*, 28–71
14. Bruce, H.M. (1959). An exteroceptive block to pregnancy in the mouse. Nature *184*, 105.
15. Fanselow, M.S., and Bolles, R.C. (1979). Naloxone and shock-elicited freezing in the rat. J. Comp. Physiol. Psychol. *93*, 736–744.
16. Cummings, K.A., and Clem, R.L. (2020). Prefrontal somatostatin interneurons encode fear memory. Nat. Neurosci. *23*, 61–74.
17. Rosenberg, M., Zhang, T., Perona, P., and Meister, M. (2021). Mice in a labyrinth show rapid learning, sudden insight, and efficient exploration. eLife *10*, e66175.
18. Dudchenko, P.A. (2004). An overview of the tasks used to test working memory in rodents. Neurosci. Biobehav. Rev. *28*, 699–709.
19. Morris, R.G.M. (1981). Spatial localization does not require the presence of local cues. Learn. Motiv. *12*, 239–260.

20. Morris, R. (1984). Developments of a water-maze procedure for studying spatial learning in the rat. J. Neurosci. Methods *11*, 47–60.
21. Sloin, H.E., Bikovski, L., Levi, A., Amber-Vitos, O., Katz, T., Spivak, L., Someck, S., Gattegno, R., Sivroni, S., Sjulson, L., et al. (2022). Hybrid offspring of C57BL/6J mice exhibit improved properties for neurobehavioral research. eNeuro *9*, ENEURO.0221-22.2022.
22. Burwell, R.D., Saddoris, M.P., Bucci, D.J., and Wiig, K.A. (2004). Corticohippocampal contributions to spatial and contextual learning. J. Neurosci. *24*, 3826–3836.
23. O'Keefe, J., and Nadel, L. (1979). Précis of O'Keefe & Nadel's The hippocampus as a cognitive map. Behav. Brain Sci. *2*, 487–494.
24. Carandini, M., and Churchland, A.K. (2013). Probing perceptual decisions in rodents. Nat. Neurosci. *16*, 824–831.
25. Burgess, C.P., Lak, A., Steinmetz, N.A., Zatka-Haas, P., Bai Reddy, C., Jacobs, E.A.K., Linden, J.F., Paton, J.J., Ranson, A., Schröder, S., et al. (2017). High-yield methods for accurate two-alternative visual psychophysics in head-fixed mice. Cell Rep. *20*, 2513–2524.
26. Aguillon-Rodriguez, V., Angelaki, D., Bayer, H., Bonacchi, N., Carandini, M., Cazettes, F., Chapuis, G., Churchland, A.K., Dan, Y., Dewitt, E., et al. (2021). Standardized and reproducible measurement of decision-making in mice. eLife *10*, e63711.
27. Marks, W.D., Osanai, H., Yamamoto, J., Ogawa, S.K., and Kitamura, T. (2019). Novel nose poke-based temporal discrimination tasks with concurrent in vivo calcium imaging in freely moving mice. Mol. Brain. *12*, 90.
28. Yu, Y., Hira, R., Stirman, J.N., Yu, W., Smith, I.T., and Smith, S.L. (2018). Mice use robust and common strategies to discriminate natural scenes. Sci. Rep. *81*, 1379.
29. Wong, A.L., Goldsmith, J., Forrence, A.D., Haith, A.M., and Krakauer, J.W. (2017). Reaction times can reflect habits rather than computations. eLife *6*, e28075
30. Olton, D.S., and Paras, B.C. (1979). Spatial memory and hippocampal function. Neuropsychologia *17*, 669–682.
31. Bernaud, V.E., Hiroi, R., Poisson, M.L., Castaneda, A.J., Kirshner, Z.Z., Gibbs, R.B., and Bimonte-Nelson, H.A. (2021). Age impacts the burden that reference memory imparts on an increasing working memory load and modifies relationships with cholinergic activity. Front. Behav. Neurosci. *15*, 610078.
32. Bimonte-Nelson, H.A., Daniel, J.M., and Koebele, S. V. (2015). The mazes. In Theories, Practice, and Protocols for Testing Rodent Cognition, H.A. Bimonte-Nelson, ed. (Humana Press), pp. 37–72.
33. Schwegler, H., Crusio, W.E., and Brust, I. (1990). Hippocampal mossy fibers and radial-maze learning in the mouse: A correlation with spatial working memory but not with non-spatial reference memory. Neuroscience *34*, 293–298.
34. Broadbent, N.J., Squire, L.R., and Clark, R.E. (2007). Rats depend on habit memory for discrimination learning and retention. Learn. Mem. *14*, 145-151.
35. Seger, C.A., and Peterson, E.J. (2013). Categorization=decision making+generalization. Neurosci. Biobehav. Rev. *37*, 1187–1200.
36. Maes, E., De Filippo, G., Inkster, A.B., Lea, S.E.G., De Houwer, J., D'Hooge, R., Beckers, T., and Wills, A.J. (2015). Feature- versus rule-based generalization in rats, pigeons and humans. Anim. Cogn. *18*, 1267.

37. Shadmehr, R., and Mussa-Ivaldi, F.A. (1994). Adaptive task of dynamics during learning of a motor task. J. Neurosci. *14*, 3208–3224.
38. Brooks, D.I., Ng, K.H., Buss, E.W., Marshall, A.T., Freeman, J.H., and Wasserman, E.A. (2013). Categorization of photographic images by rats using shape-based image dimensions. J. Exp. Psychol. Anim. Behav. Process. *39*, 85–92.
39. Broschard, M.B., Kim, J., Love, B.C., Wasserman, E.A., and Freeman, J.H. (2019). Selective attention in rat visual category learning. Learn. Mem. *26*, 84–92.
40. Levi, A., Spivak, L., Sloin, H.E., Someck, S., and Stark, E. (2022). Error correction and improved precision of spike timing in converging cortical networks. Cell Rep. *40*, 111383.
41. Senzai, Y., and Scanziani, M. (2022). A cognitive process occurring during sleep is revealed by rapid eye movements. Science *377*, 999–1004.
42. Sloin, H.E., Levi, A., Someck, S., Spivak, L., and Stark, E. (2022). High fidelity theta phase rolling of CA1 neurons. J Neurosci. *42*, 3184-3196.
43. Voitov, I., and Mrsic-Flogel, T.D. (2022). Cortical feedback loops bind distributed representations of working memory. Nature *608*, 381–389.
44. Rogers, S., Rozman, P.A., Valero, M., Doyle, W.K., and Buzsáki, G. (2021). Mechanisms and plasticity of chemogenically induced interneuronal suppression of principal cells. Proc. Natl. Acad. Sci. USA. *118*, e2014157118.
45. Tarnavsky Eitan, A., Someck, S., Zajac, M., Socher, E., and Stark, E. (2021). Outan: An on-head system for driving µLED arrays implanted in freely moving mice. IEEE Trans. Biomed. Circuits Syst. *15*, 303–313.
46. Sadtler, P.T., Quick, K.M., Golub, M.D., Chase, S.M., Ryu, S.I., Tyler-Kabara, E.C., Yu, B.M., and Batista, A.P. (2014). Neural constraints on learning. Nature *512*, 423-426.
47. Pakan, J.M.P., Francioni, V., and Rochefort, N.L. (2018). Action and learning shape the activity of neuronal circuits in the visual cortex. Curr. Opin. Neurobiol. *52*, 88–97.
48. Poort, J., Khan, A.G., Pachitariu, M., Nemri, A., Orsolic, I., Krupic, J., Bauza, M., Sahani, M., Keller, G.B., Mrsic-Flogel, T.D., et al. (2015). Learning Enhances Sensory and Multiple Non-sensory Representations in Primary Visual Cortex. Neuron *86*, 1478–1490.
49. Jurjut, O., Georgieva, X.P., Busse, L., and Katzner, S. (2017). Learning enhances sensory processing in mouse V1 before Improving behavior. J. Neurosci. *27*, 6460-6474.
50. Lak, A., Okun, M., Moss, M.M., Gurnani, H., Farrell, K., Wells, M.J., Reddy, C.B., Kepecs, A., Harris, K.D., and Carandini, M. (2020). Dopaminergic and prefrontal basis of learning from sensory confidence and reward value. Neuron *105*, 700-711.
51. Le Merre, P., Esmaeili, V., Charrière, E., Galan, K., Salin, P.A., Petersen, C.C.H., and Crochet, S. (2018). Reward-based learning drives rapid sensory signals in medial prefrontal cortex and dorsal hippocampus necessary for goal-directed behavior. Neuron *97*, 83-91.
52. Chevée, M., Finkel, E.A., Kim, S.J., O'Connor, D.H., and Brown, S.P. (2022). Neural activity in the mouse claustrum in a cross-modal sensory selection task. Neuron *110*, 486-501.
53. Stark, E., Koos, T., and Buzsáki, G. (2012). Diode probes for spatiotemporal optical control of multiple neurons in freely moving animals. J. Neurophysiol. *108*, 349–363.
54. Gaspar, N., Eichler, R., and Stark, E. (2019). A novel low-noise movement tracking system with real-time analog output for closed-loop experiments. J. Neurosci. Methods. *318*, 69–77.

55. Rossant, C., Kadir, S. N., Goodman, D. F. M., Schulman, J., Hunter, M. L. D., Saleem, A. B., Grosmark, A., Belluscio, M., Denfield, G. H., Ecker, A. S., et al. (2016). Spike sorting for large, dense electrode arrays. Nat. Neurosci. *19*, 634–641.